

## Co-linear study between the effective Band Mass in a solid and free electron mass with reference to Kronig-Penney Model

Miss.Supriya Lahanbhau Dengale

SMBST, Arts, Science & Commerce College, Sangamaner

### Abstract

A model used to look at the characteristics of electrons trapped in a periodic function is Model Kronig-Penney. This model is useful due to the fact that Bloch's theorem permits an analytical look at the electronic proper ties. The electron's powerful mass is a key concept that effects the resulting electron band principle. The so-called powerful mass theorem," which we follow in the Kronig-Penney model, permits us to ask and reply to the subsequent questions: to what extent does the powerful electron mass rely on the mass of free electrons in addition to the residences of the recurring potential? With this principle and specific computations using the Kronig-Penney paradigm, we reveal the transition from a weak recurring state capability to a strong periodic capability. This paper additionally addresses the unique scenario of the Dirac-comb model. Among other subjects, we show, using the powerful mass theorem, that an imbalance inside the hundreds of electrons and holes is often anticipated, although electron-electron interactions are not present to contribute.

**Keywords:** *Powerful mass, Bloch's theorem, Kronig-Penney model, electron band principle, periodic potential and effective mass theorem*

### Introduction

Free electrons have many traits in common with itinerant electrons in materials. In other words, they possess mass, often include a bad charge  $-e$ , and regularly display a parabolic wave-vector dispersion. Specifically, this latter reality indicates that strong-country electrons are certainly loose electrons, with the exception that the inverse unfastened electron mass frequently does not decide the curvature in any given route. As a result, electrons seem to be free," however, they truly have a "powerful" mass. This is special because of their electron mass. Thus, one could wonder: What factors affect its mass? Since the debris are electrons, one would count on the fact that the band mass and electron mass are connected. In comparison, a strong structure is formed by a recurring pattern of ions whose attractive properties act as centres for attracting specific electrons (by focusing on just one electron, we are able to bypass the very difficult issue of interacting electrons). As a result, the tunnelling system—in which basically constrained states become prolonged—is how the electrons act in the fabric. Therefore, it makes sense that the band mass would be extraordinarily dependent on the size of those tunnelling boundaries, which in turn will depend on the fabric's structure (along with lattice spacing).

These are exceptional factors of view; the solution is normally known (though perhaps now not as well called it has to be!), as we give an explanation for below. It is made up of the two outcomes noted in the preceding section combined. The purpose of the article is to specificize this issue in a single category, in addition to using the renowned Kronig-Penney paradigm to do so.

The Kronig-Penney version simulates Coulombic potentials on the atomic degree, located in a real setting thru using a finite square nicely array in a single measurement. Understanding electric bands and finding the satisfactory explanation for why positive materials are metals at the same time as alternatives may be insulator is facilitated by using this model. The analytical or numerical solution of the Kronig-Penney model, using Bloch's theorem, is important for explaining how electrons pass within a recurring array.

According to Bloch's theorem, an electron's eigenstates for a periodic ability are made from products of aircraft waves and a position-dependent function that has the same periodicity as the potential. That is, eigenstates of the form  $\psi(x) = e^{ikx} u(x)$ , where  $u(x) = u(x)$ , with  $\psi(x)$  representing the wave characteristic describing the electron, and  $\Lambda$  is the period of the array of ions' periodicity. This can also be written as:

$\varphi(x + 1) = e^{ik\Lambda} \varphi(x)$  Consequently,

$$\varphi_k(x + 1) = e^{ik\Lambda} \varphi_k(x) \quad (1)$$

The simplest difference between these equations is that the second has a subscript referred to as "asokay" appended to the wave functions, wherein  $k$  is a wave vector,  $-\pi < k < \pi$ . We must effectively point out the wave vector  $k$  within the 2D equation for the reason that the initial formula is the source of the brand new quantum variety. Bloch's theorem essentially permits us to do a much simpler computation beyond a single unit cell, involving only a single ion potential. This derivation enables the characterization of electron wave functions that span throughout the entire solid. As we'll see, an index 'n,' or second quantum range, will quickly emerge and be used to list the eigenvalues and eigenstates in additional elements. The formation of electron bands is proven with the aid of an evaluation of the analytical approach to the Kronig-Penney version, which is generally well-known to show parabolic dispersion close to  $0k = \text{zero}$  and  $k = \pi/\Lambda$ . The effective mass,  $m^*$ , that electrons accumulate because of this parabolic dispersion is the mass that electrons appear to have while they're stable. We refer to the bottom and pinnacle of every band, which are often domestic to the parabolic dispersion because of the electron as well as the hole effective mass. The electricity dispersion at those extreme webpages can be roughly described as parabolic. Making use of these facts yields the only-dimensional equation that connects the powerful mass to the dispersion curve's curvature:

$$\frac{1}{m_{kn}} = \frac{1}{\hbar^2} \frac{d^2 E_{kn}}{dk^2} \quad (2)$$

wherein the power from the nth strategy to the equation, if you want it to be defined later, is now indicated with the aid of the inclusion of the n subscript. These formulations control a solid's band shape, as defined via the Kronig-Penney model. Please take notice that, for the sake of simplicity, we can only be discussing one dimension in this article. We think that senior college

undergraduates and graduates taking their initial path in condensed depend physics will locate the content material in this text without problems in its contemporary layout. More superior textbooks offer a more precise treatment of the band shape and specific measurable observables of actual three-dimensional materials. Equation (2) offers us the answers, so we are able to use smooth differentiation to get the electron's powerful mass band by using the band, although in the case of a potential more intricate than that of a square well. However, equation (2) ignores the truth that the strength ranges in other bands exert a few constraints on the powerful mass of a selected band. This is made clear within the powerful mass equation that follows, which's was derived. Well, it's far

$$\frac{1}{m_{kn}} = \frac{1}{m_e} + \frac{2}{m_e^2} \sum_{n' \neq n} \frac{|kn|p||kn|}{E_{kn} - E_{kn'}}^2 \quad (3)$$

where  $m_e$  is the mass of the free electron,  $\hat{p} = -i \hbar \nabla$  is the momentum operator, and  $|kn\rangle$  is the Bloch state with wave vector  $k$  in the  $n$ th band. When applied to optical measurements, this is commonly known as the f-sum rule or the effective mass theorem.

When equation (3) is closely examined, it can be seen that it straddles the two diametrically opposed concepts introduced in the initial paragraph. The effective mass in the weak potential limit is by the mass of free electrons, this implies that, to ensure no tunnelling barrier obstructs the flow of electrons from "atom" to "atom," only the first term on the right-hand side (rhs) of equation (3) contributes as the depth of the square wells gets closer to zero." On the other hand, in the strong potential limit, the second term on the right side of equation (3) predominantly yields the result. The free electron mass and the effective mass are only tangentially related when the tunnelling barriers are extremely big (high or broad). Actually, even these claims are not really clear from equation (3), as just the wave function and energy—that is, the solutions—are displayed on the right side of the equation in relation to the band configuration issue, not the specifics of the barrier heights and widths. It's interesting to note that both components in equation (3), since the wave function is a product,  $\psi_k(x) = e^{ikx} u_k(x)$ , can be viewed as contributions from each of these terms. The second part in equation (3) is derived from the  $u_k(x)$  portion, whereas  $e^{ikx}$ , the plane wave component, is what causes the  $1/m_e$  contributions. It seems that a wave function of the product generates "transmission" amplitudes within a chain.

Equation (3) also has the important consequence of showing that various bands in solids meet constraints among themselves in an interconnected manner. Any numerical computation will automatically satisfy these limitations. Nonetheless, basic models are often constructed by examining a few relevant bands near the Fermi level. Prototypes may be allowed to let parameters fluctuate on their own with only one band. However, equation (3) places restrictions on the model parameters when there are two or more bands. Although this limitation may not be as severe, it has undoubtedly been disregarded in the majority of computations employing basic models.

The result of equation (3) is that for all barrier strengths, the following term on the RHS for the hole's effective mass must be negative. Only at the extremely strong limitation, sometimes considered to be the limit of rigid binding, can electron-hole symmetry be reached. At that point, the hole's effective mass approaches the effective mass of an electron in magnitude, however, with the opposite indication. The second term on the RHS diverges in the "free" hole limit, and  $m^*$  becomes closer to 0 (from the negative side). These factors lead us to believe that, given a model for which analytical methods can be used for at least some of the energy band calculations, it is helpful to look closely at equation (3). One model that has been around for over ninety years is the Kronig-Penney model. Further analytical findings may be obtained by introducing a simplified form, also referred to as the Dirac comb model, in the next section. The Kronig-Penney model's effective mass results are given in the study; although they are numerically required, they are readily attainable by undergraduate students.

### Kronig–Penney Framework

According to the Kronig-Penney version, an electron moves in a periodic capacity as shown in fig 1, and wells using a width  $w$  and a lattice spacing of  $= w b$  are divided by using alternating capability obstacles of width  $b$  and height  $V_0$ . The square wells represent atomic centres in a strong, vague manner. When it involves atoms with excessive  $Z$  atomic numbers, those wells may go rather deep. This suggests that there can be robust limitations isolating those wells; as a robust barrier inside the Kronig-Penney version may be represented with the aid of a large width and a vast peak, we are able to study features on the subject of both barrier attributes. In the stop, the tunnelling amplitude will determine the strength" of a barrier. Constrained dispersion and a high effective mass are the outcomes of a low tunnelling amplitude. Mathematically, the complete ability is represented as follows:

$$V(x) = V_0 \sum_{n=-\infty}^{\infty} \theta[x - (nl - b)]\theta[nl - x] \quad (4)$$

The Heaviside step feature is represented by using  $\theta[x]$ . For each vicinity within the unit mobile, the Schrödinger equation needs to be solved so that it will determine the energy-containing states beneath the barriers  $V_0$  and  $E$ . For the nicely, this means solving a linear combination of aircraft waves, and for the barrier area, it means solving a linear mixture of exponentially growing and decaying features. Bloch's theorem is used to provide the boundary conditions so that the solution may also circulate from one unit mobile to the next. Four coefficient-containing linear homogeneous equations are acquired by corresponding with the wave characteristic as well as its offshoot at the interfaces; those equations can be expressed in matrix form. The determinant of the matrix needs to be the same zero in order for there to be a nontrivial answer; this turns into the formula that specifies the permitted energy.

$$\cos(kl) = \cos(k_1\omega) \cosh[k_2b] + \frac{k_2^2 - k_1^2}{2k_1k_2} \sin(k_1\omega) \sinh(k_2b) \quad (5)$$

Wherein the solutions for every cost of  $k$  are indexed in the  $n$  subscript, which has been suppressed, Where  $k_1 = \sqrt{2mEk}/\hbar$  and  $k_2 = \sqrt{2m(V_0 - Ek)}/\hbar$ . Transcendental equation (5) has solutions  $E_{kn}$ , which need to be found numerically. Typically, the subscript  $n$  is called the band index. In fact, the process of fixing equation (5) involves selecting a price for  $E$ , identifying  $k_1$  and  $k_2$ , and then evaluating the rhs of the equation, whose absolute cost is either larger or much less than harmony. If this range is bigger, then it is apparent that no solution is achievable; if it is less than team spirit, then the value of okay for which this power is the answer can be observed by way of calculating the inverse cosine of this quantity. This method offers an okay for a given  $E$  instead of answering the unique query, what is  $E$  for a given okay? Iteration isn't always necessary in this manner, and the identical effects are obtained. Likewise, if  $E$  is greater than  $V_0$ , we get,

Similarly, when  $E > V_0$ , we obtain

$$\cos(kl) = \cos(k_1\omega) \cos[k_2b] - \frac{k_2^2 - k_1^2}{2k_1k_2} \sin(k_1\omega) \sin h(k_2b) \quad (6)$$

**Figure 1. The periodic potential of the Kronig-Penney model is represented by wide wells (w), strong barriers (b), and barrier heights (V0).**

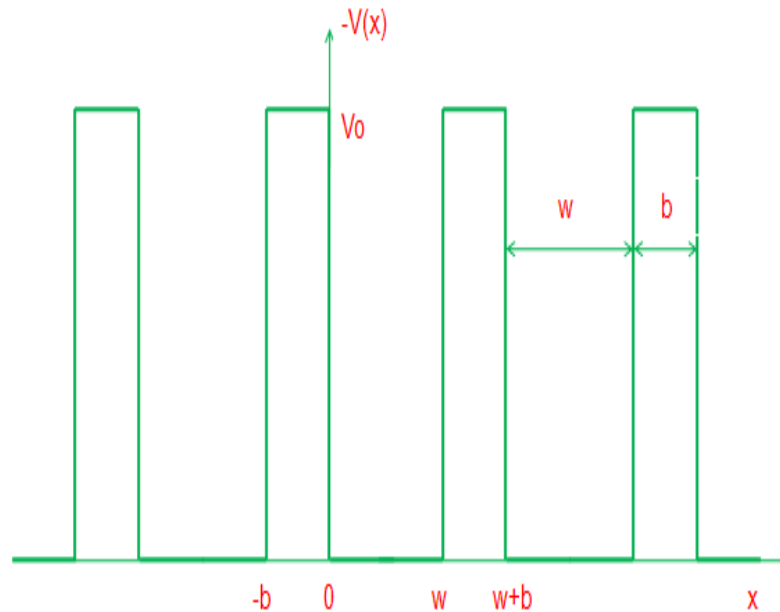


**Figure 2. The graph shows the solution to equations (5) and (6) for values of  $v_0 = 200$  and  $b/ = 0.1$ . The limits of the  $\cos(k)$  range are represented by two horizontal lines and the RHS by a solid red curve.**

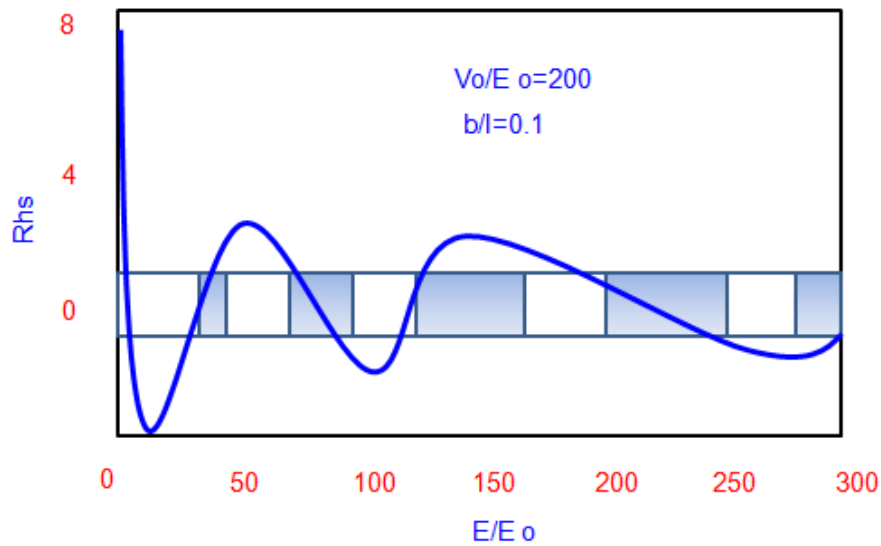
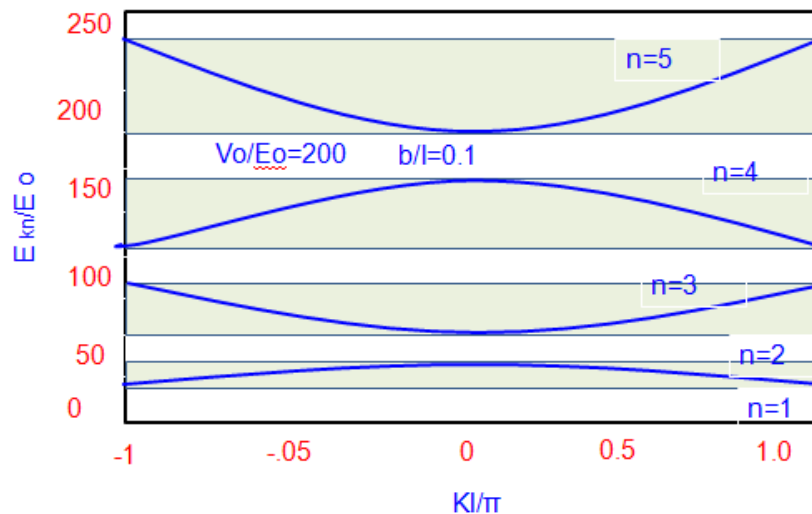


Figure 3. The band structure of the Kronig-Penney model, with parameters  $v_0 = 200$  and  $b/l = 0.1$ , displays the first five of an infinite number of solutions with an index 'n'.



Wherein the other numbers remain identical and  $k_2 = \sqrt{2m(E_k - V_0)}/\hbar$ . The solutions were acquired as previously stated. Plotting the rhs as a function of E may be used to visually represent the answers to equations (5) and (6). This is shown in Figure 2 for a selected selection of b and  $V_0$  (represented by the stable red curve). We use the dimensionless barrier peak  $v_0 = V_0/E_0$  and the normalised barrier width, b/l, to characterise the capability choice because we adopt electricity devices of  $E_0 \equiv 2/(2me^2)$ . Every segment of the sinuous curve positioned between 1 and  $-1$  has a continuum of solutions, and the shaded location suggests that  $ok$  degrees are between 0 and  $\pm\pi$ , respectively. It is evident that there are not any answers when the RS has an absolute fee greater than team spirit. Plotting the low electricity answers received this way as



Ek<sub>n</sub> vs. Ok in Figure 3 makes it clear that bands are gifts and are separated by way of strength gaps. The structure of this band is included in a few textbooks in addition to current, in citations. Specifically, the bands have a tendency to be parabolic within the vicinity of k = zero and ok = π/, displaying minima or maxima at those wave vectors. By becoming a parabola to the findings proven in parent 3, as proven in reference, the powerful mass may be easily retrieved at those locations. We have an additional alternative given via equation (3): We may additionally calculate the powerful mass at k = zero (or ok = π/) by way of adding up a feature across the alternative bands on the same vector of waves. This newsletter contains: We intend to take a better look at this equivalency. But first, we provide an extra-truthful model, wherein some of the algebra is less difficult to apprehend.

### Dirac comb model

Because extra analytical findings are available, the Dirac comb model, a simplification of the Kronig-Penney model, is regularly addressed in undergraduate literature in preference to the Kronig-Penney model. We will stray from our subject matter for a second and say that this additionally applies to the powerful mass theorem. For b → 0 and V0 → ∞, this version is the proscribing case of the Kronig-Penney version, such that bV0 ≥ α remains constant. In other words, the distances between wells emerge as regularly smaller and taller. As a result, one gets a series of δ-characteristic potentials in place of a series of obstacles with restricted width.

$$V(x) = \sum_{n=-\infty}^{\infty} \alpha \delta(x - nl) \quad (7)$$

And ω = l. Using z ≡ k<sub>1</sub>l ≡ √(2m<sub>e</sub>E/h<sup>2</sup>l) ≡ √(E/E<sub>0</sub>), the energies' governing equation, which is fully contained in z, is

$$\cos(kl) = \cos z + \beta \frac{\sin z}{z} \quad (8)$$

Where β is an unmarried parameter proportionate to the barriers' power, and meα / 2 = β. Compared to equations (5) and (6), equation (8) is easier to see (as a characteristic of z). Despite this, the rhs is much like the only in parent 2, but it's now displayed as a characteristic of z ⊥ √E in place of E. More notably, half of the solutions can be easily found analytically. For example, each 2nd answer can be determined analytically for ok = ±π and k = zero with the aid of the use of z = (2m - 1)π and z = 2mπ, respectively, where m is a fine integer. Equation (8)'s rhs as a feature of z is proven in the study, which additionally affords an excellent instance of the analytical solutions. Equation (eight) is easy, hence the powerful mass on the band's extrema can be decided analytically with the use of this honest system:

$$\frac{m_e}{m_k} = \frac{z \cdot \cos(kl)}{\sin z + \frac{\beta}{z} (\frac{\sin z}{z} - \cos z)} \quad (9)$$

Equation (8)'s feature for  $\beta = 6$ . The rhs of equation (8) is represented by the stable (crimson) curve as a function of  $z/\pi = E/E_0/\pi$ . The obstacles of the  $\cos(ok)$  variety, proven with the aid of the two horizontal dashed (black) strains, are  $-1$  and  $1$ . The sections of the solid crimson curve between  $-1$  and  $1$ , or amidst the two horizontal strains, are the answers to equation (eight), as proven in parent 2. These parts create bands of probably different energy that are contrasting with each other by gaps in energy. Analytical solutions for the Dirac comb version are viable and are proven via blue squares for  $ok = 0$  at  $z = \pi, 4\pi,$  and  $6\pi$ , and with the aid of mauve circles for  $k = \pi/$  at  $z = \pi, 3\pi,$  and  $5\pi$ .

Effective mass for the hole at  $k = \pi/$  (blue curve with blue circle factors) and the electron at  $k =$  zero (pink curve with crimson rectangular factors) for the Dirac comb hassle's lowest strength band ( $n = 1$ ). Equation (nine) yields the curves, while equation (3) yields the factors (the specifics of this computation. Equation (10) also yields the hollow effective mass end result for  $n = 1$ . The modest  $\beta$  result produced via equation (eleven)—where  $z$  is derived from the answer of equation (8)—is also shown (dashed curve on the origin). There are a few barriers to how this equation can be accelerated. For instance, the  $n$ th band's hole-like, powerful mass is furnished by means of

$$\frac{m_e}{m_{kn}} = -\frac{(n\pi)^2}{\beta} \quad (10)$$

wherein, for even values of  $n$ ,  $ok = 0$  and, for abnormal values of  $n$ ,  $ok = \pi/$ . This formula works for any value of  $\beta$ . The effective mass for dimensionless wave vector okay in band  $n$  is indicated by using the notation  $m^* kn$ ; so, the conclusion for  $k = \pi/$  inside the first band is  $m_e/m^* \pi 1 = -\pi^2/\beta$ . Specifically, this cost diverges as  $\beta \rightarrow 0$ , the electricity of the limitations. This is an exciting restriction due to the fact that, under the circumstance that the dispersion methods the zero-slope Brillouin zone border ( $\pm\pi/$ ), we assume it to method a free electron-like parabola. The effective mass resulting from this restriction is sort of nil. Naturally, in the meantime, the powerful mass at  $k =$  zero approaches the mass of the unbound electron. Indeed, it could be shown that, for the lowest band,

$$\frac{m_e}{m_{01}} \approx \frac{1}{1 + \frac{\beta}{45}} (\beta \rightarrow 0) \quad (11)$$

Simple algebra demonstrates that in the situation of  $k = 0$  for extremely large barriers ( $\beta \rightarrow \infty$ )

$$\frac{m_e}{m_{01}} \approx \frac{\pi^2}{\beta} (\beta \rightarrow \infty) \quad (12)$$



This, when assessed for the lowest band in equation (10) for all values of  $\beta$ , is symmetric with the end result for the hole ( $ok = \pm\pi$ ). Given that this is a specific situation concerning  $\delta$ -characteristic obstacles, those conclusions that have an algebraic reliance on the barrier strength,  $\beta$ , are instead deceptive. Generally, there is an exponential dependence on barrier height as well as width measurements. The electron-hollow mass symmetry (inside a particular band) is, however, handiest present at the extreme huge barrier restriction, also called the tight-binding restriction, as proven via the simplified Dirac comb model. The electron mass is greater than the hollow mass for small obstacles (also referred to as the unfastened electron" restriction), and that is real for all intermediate barrier strengths, as we will discover within the subsequent section. This presents the effective mass of the electron ( $ok = \text{zero}$ ) and hollow ( $ok = \pi$ ) for the first band ( $n = 1$ ) as a feature of  $\beta$ . Additionally, we provide the results of equation (three) (points), which obviously correspond with the effects of equation (9) (curves). The modest  $\beta$  result provided through equation (11) is also shown. It consists of the specifics of the computation performed using equation (three). These summations can honestly be finished analytically for the Dirac comb, which is a good way to get equation (9); however, in this case, we just perform the sum numerically. This enables us to investigate the convergence of equation (three) as a function of the encompassing bands and ascertain the features that different bands perform within the machine. As we move back to the findings for the entire Kronig-Penney model, we do this within the element that follows.

### Outcome for the Kronig–Penney Framework

Equation (2) illustrates a way to get an appropriate effective mass with the aid of thinking about two derivatives of the electricity with respect to  $ok$ . Additionally, we determine the powerful mass by finishing the summation needed to fulfil equation (three); in reality, this results in a finite sum of as much as  $n_{\text{max}}$ . It is important to analyse the relationship between this sum's convergence and the barrier strengths. More drastically, this well-known statistic shows the degree of interdependence between the one-of-a-kind bands.

The powerful electron mass for the bottom electricity band for more than a few barrier strengths is shown in Discern 6. We graph the powerful mass ( $n_{\text{max}}$ ), or the quantity of bands maintained inside the sum, as a feature of the wide variety of bands in equation (3). As  $n_{\text{max}}$  grows, those findings inevitably converge to the final results produced by using equation (2), which is shown by way of a horizontal line. As additional terms are delivered to the sum, the effective mass that is derived from the whole tactic is the actual result in a monotonic manner. The study illustrates that, for surprisingly low obstacles, practically the best one-time period is wanted; that is, there are regulations on the effective parameters that may be hired to characterise a primary two-band model. More words are wanted, but as  $v_0$  rises, Also, be aware of the reality that certain bands do not pay tribute; as an example, the third and fifth bands upload quite little when  $v_0 = \text{four hundred}$  is blanketed. Analytically, it is easy to illustrate that that is the case for each second band within the Dirac comb model. Although a computational analysis for the complete Kronig-Penney version has no longer been possible, we get numerically equal conclusions.

In the study, we have used a barrier width of  $b/l = 0.2$ . The qualitative outcomes for exceptional barrier widths confirm expectations: results with wider limitations resemble people with narrower limitations, but with a touch of large barrier capacity. The barrier strengths listed here

are probably no longer sensible. Given that the powerful mass for the lowest degree is displayed, or a so-called centre nation," the powerful loads frequently get pretty large. Since these electrons are not in any respect itinerant in a stable (see sodium's 1 s state as an example), their effective mass is in reality limitless. Specifically, in the study, the electron-power mass ratio is always greater than unity. The 2D aspect in equation (3) will definitely make contributions if we observe better strength bands, and the powerful electron mass ratio may also drop below harmony. This was accomplished, wherein potentials of various shapes were additionally tested. It gives an instance to illustrate this behaviour. Here,  $b/ = \text{zero.2}$  and  $v_0 = 1000$  are used. We looked at the electron-like okay = 0 minimal for this barrier strength for the first five bands with powerful mass ratios ranging from 278 to 0.13. We have used a logarithmic scale due to the large fluctuation, despite the fact that the effective hundreds are shown in the photograph itself. The possibility of effective loads that are smaller than the loose electron mass should be particularly noted, as this is often the case in real substances.

On wide consideration, electron-hollow imbalance is anticipated. The hole part of the band, closer to the barrier's top than the electron element, has smaller effective numbers due to a lower-strength barrier. Some experts conducted an analytical analysis of this, and the pattern proven here is steady with that evaluation: a high degree of asymmetry at small boundaries and an upward push in symmetry with growing barrier length

## Conclusion

The effective mass theorem," which distinguishes between the band and loose electron contribution to the powerful mass of electrons and describes an electron visiting the interior as having a periodic capability, has been offered. More complex computations might also enjoy the use of this theorem, in particular when numbers for a certain wave vector (okay, = 0, as an instance) are less complicated to get than the ones over many wave vector combinations. In this study, we investigated the results of this method for the Kronig-Penney version, a one-dimensional easy periodic capability. In the lowermost electricity band, we managed to absolutely show that the powerful mass is ruled by using the free electron mass within the maximum value of low barrier heights, while the effective mass is mainly determined by using the tunnelling method through these limitations when big barriers are present. For electron-like vendors (electrons with power at the bottom of a band) and hole-like vendors (electrons with energy in the direction of the pinnacle of a band), an herbal imbalance results from the contribution of both of these capabilities to the electron effective mass. Due to the reality that the barrier potential is more closely approached by hole energies than by electron energies, the latter have lower powerful loads than the former for a given band. As a result, their effective mass is reduced because of a bigger tunneling amplitude and elevated dispersion. The imbalance inside the powerful mass of electrons and holes may also have considerable implications for semiconductors and superconductors. For metals and superconductors, it is common practice to expect electron-hole symmetry from the outset and credit any growing asymmetries to interactions by myself. However, our discovery increases the opportunity that single particle functions might be answerable for some portion of the electron-hole asymmetry. All those observations also hold for patterns in higher dimensions; the possibility of overlapping electricity, as one might anticipate bands with so-referred to as indirect spaces leads to captivating science in better dimensions, which has determined applications in electronics.

However, in each of the three dimensions, the fundamental weak barrier ability as well as strong barrier capacity obstacles hold true. In fact, there have already been computations for a three-dimensional machine that do not employ the effective mass assumption.

**References:**

1. Ashcroft, N. W., & Mermin, N. D. (1976). Solid state physics. Holt, Rinehart and Winston.
2. Baldereschi, A., & Mahan, G. D. (1984). Fundamentals of thin films and heterostructures. World Scientific.
3. Bardeen, J., Cooper, L. N., & Schrieffer, J. R. (1957). Theory of superconductivity. Physical Review, 108(5), 1175.
4. Bastard, G. (1998). Electrons in semiconductor heterostructures. Wiley-VCH.
5. Bezares, R. G., & Mostofi, A. A. (2023). Materials science with ab initio electronic structure methods. Cambridge University Press.
6. Bloch, F. (1928). Über die quantenmechanik der elektronen in kristallgittern. Zeitschrift für Physik, 58(6), 593-603.
7. Cohen, M. L. (1971). The electronic structure of solids: An introduction for physicists. Springer-Verlag.
8. Dresselhaus, G., & Dresselhaus, M. S. (1982). Spin-splitting in semiconductor heterostructures. Journal of Physics C: Solid State Physics, 15(25), 5173.
9. Kittel, C. (2004). Introduction to solid state physics. Wiley.
10. Kohn, W. (1996). Electronic structure calculations for materials and molecules. Reviews of Modern Physics, 68(1), 125.
11. Kronig, R., & Penney, W. G. (1931). Quantum mechanics of electrons in crystal lattices. Proceedings of the Royal Society of London. Series A, 130(826), 601-624.
12. Mahan, G. D. (2000). Condensed matter physics. Wiley.
13. Nelson, D. F., & Park, S. (2004). Elementary solid state physics. Princeton University Press.
14. Slater, J. C. (1952). The electronic structure of molecules and solids. McGraw-Hill.
15. Tsu, R., & Gossard, A. C. (1978). Superlattice semiconductor heterostructures. Applied Physics Letters, 32(5), 285-287.